

A Rh(I)-Catalyzed Cascade Cyclization of 1,5-Bisallenes and Alkynes for the Formation of *cis*-3,4-Arylvinyl Pyrrolidines and Cyclopentanes

Jordi Vila,^a Roger Vinardell,^a Miquel Solà,^a Anna Pla-Quintana,^{a,*} and Anna Roglans^{a,*}

^a Institut de Química Computacional i Catàlisi (IQCC) and Departament de Química, Universitat de Girona (UdG), Facultat de Ciències, C/Maria Aurèlia Capmany, 69, 17003 Girona, Catalunya, Spain
E-mail: anna.plaq@udg.edu; anna.roglans@udg.edu

Manuscript received: June 28, 2021; Revised manuscript received: October 13, 2021;
Version of record online: ■■, ■■■



Supporting information for this article is available on the WWW under <https://doi.org/10.1002/adsc.202100934>

Abstract: The cascade cyclization reactions of 1,5-bisallenes grant access to a great variety of products by precisely tuning the catalyst system and/or the reagents involved. Herein, we present our findings that 1,5-bisallenes react with two molecules of dimethyl acetylenedicarboxylate to afford, in a completely diastereoselective manner, *cis*-3,4-arylvinyl pyrrolidines and cyclopentanes. DFT calculations have been used to postulate a mechanism for the developed reaction which encompasses a [2 + 2 + 2] cycloaddition reaction of the two alkynes and the external double bond of one allene, followed by a cycloisomerization involving the internal double bond of the second allene.

Keywords: Cyclization; 1,5-Bisallenes; Alkynes; Density Functional Calculations; Rhodium

Introduction

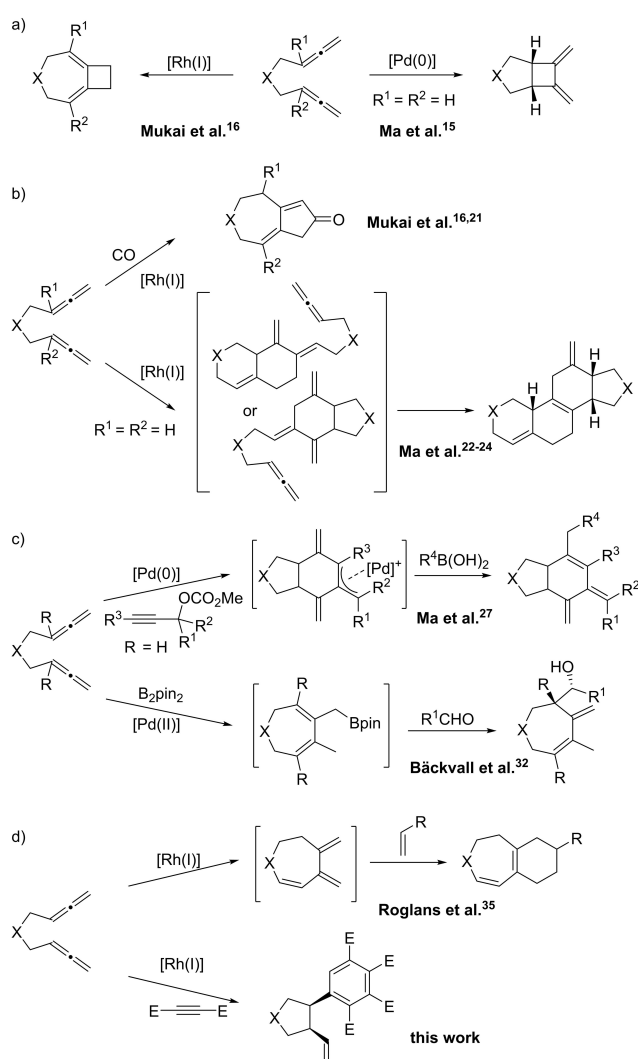
The high degree of unsaturation of allenes, spreading over three contiguous carbons, provides them with unique reactivity patterns^[1–2] especially in transition-metal mediated reactions. Although remarkable progress has been made to control the chemo-, regio- and diastereoselectivity of certain processes,^[3–11] new reactivity patterns are still to be discovered by reversing the selectivities already observed and/or by exploring cascade processes.

1,5-Bisallenes have emerged as an interesting platform to develop cycloisomerization and cyclization reactions. The main reason for this is that a great

variety of carbo- and heterocyclic skeletons can be accessed from these substrates by finely controlling the selectivity of the various reactions in which they participate.^[12–14]

Cycloisomerization reactions of 1,5-bisallenes have been shown to provide bicyclic cyclobutanes by [2 + 2] cycloaddition. Tail-to-tail cycloadducts are obtained under thermal conditions as shown by Ma et al.^[15] or under rhodium catalysis as reported by Mukai et al.^[16] (Scheme 1a). On the other hand, head-to-head cycloadducts were obtained by Ma et al.^[15] under palladium catalysis (Scheme 1a), by Nishida et al.^[17] under nickel catalysis and by Kang and Chung et al.^[18] under gold catalysis. It should be noted that in the last case a flipped cycloisomer was formed. Alternatively, rhodium catalysis has also promoted the formation of cycloisomeric 1,2-dimethylenecycloheptene scaffolds as shown by Ma et al.^[19] and Mukai et al.^[16]

1,5-Bisallenes also engage in Pauson-Khand like [2 + 2 + 1] cycloaddition reactions under heterobimetallic cobalt/rhodium or rhodium catalysis as shown by the groups of Chung^[20] and Mukai,^[16,21] respectively. In both cases, fused 5,7-membered rings were obtained, an aspect that the authors explained by involving both of the distal double bonds of the allene moieties in the oxidative cyclization (Scheme 1b). In contrast, Ma et al.^[22–24] described the bimolecular reaction of 1,5-bisallenes under a rhodium-catalyzed [2 + 2 + 2] cycloaddition, followed by an intramolecular Diels-Alder reaction to generate steroid derivatives. In this process, either the two internal (or one internal and one external) double bonds of the allene participate in the initial oxidative cyclization to afford fused 5,5- (or 5,6-) bicyclic intermediates comprising an exocyclic diene motif that readily engage in the Diels-Alder reaction (Scheme 1b).



Scheme 1. Examples of transition-metal catalysed reactions of 1,5-bisallenes.

Group 10 transition metals, especially palladium, catalyse the cyclization of 1,5-bisallenes to a variety of different scaffolds. In the key step of these transformations an organometallic species, generated *in situ* by a reaction on one allene, induces the cyclization by carbometallation to a double bond of the second allene. In this way, the mechanistic manifold intricately combines different reactions in what can be defined as cascade processes. Here again, the size of the ring formed upon carbometallation depends on the catalytic system used. Processes in which the two inner bonds of the two allenes forge 5-membered rings have been described under palladium catalysis by Kang et al.,^[25] Yu et al.^[26] and Ma et al.,^[27–28] (Scheme 1c) under platinum catalysis by Jang et al.,^[29] and under nickel catalysis by Arai et al.^[30] Conversely, cyclizations involving the two external double bonds, thus affording 7-membered scaffolds, have been reported by

Bäckvall et al.^[31–32] under palladium catalysis (Scheme 1c) and by Muñoz et al.^[33] under platinum catalysis. Ma et al.,^[34] using a reaction manifold that does not directly react the two allenes, also obtained 10-membered macrocycles.

Our group recently developed a cascade reaction involving 1,5-bisallenes and alkenes,^[35] including C₆₀,^[36] to obtain fused 6,7-membered rings (Scheme 1d). The mechanism is postulated to proceed via an initial rhodium-catalysed cycloisomerization of the bisallene leading to a non-isolable 1,2-dimethylenecycloheptene scaffold, followed by a regioselective Diels-Alder reaction with alkenes in which the rhodium does not participate. The precedents of 1,5-bisallene reactivity summarized above nicely show that these are excellent scaffolds for transition-metal catalysed cascade processes, in which small variations in the catalyst or the reagents have a profound impact on the products obtained. Furthermore, in rhodium-catalysed cycloaddition reactions it is known that alkynes are much more reactive than alkenes, and that the reactivity of allenes falls somewhere between the two.^[37–39] Thus, as a continuation of our programme based on the development of rhodium-catalysed cycloadditions involving allenes,^[35–38,40–42] we asked ourselves what the favoured reaction pathway would be if we treated 1,5-bisallenes with alkynes under rhodium catalysis. We reasoned that the greater reactivity of alkynes as compared to alkenes might favour a fully rhodium catalysed cascade process. We have now performed these reactions and report here that, as predicted, a new cyclization reaction prevailed that encompasses a rhodium-catalysed [2+2+2] cycloaddition between two alkynes and one allene unit followed by a cycloisomerization involving the second allene of the bisallene to diastereoselectively generate *cis*-3,4-arylvinyl pyrrolidine and *cis*-3,4-arylvinyl cyclopentane derivatives.

Results and Discussion

We initially chose to evaluate the reaction between *N*-tosyl-tethered 1,5-bisallene **1a** and dimethyl acetylenedicarboxylate (DMAD) **2a** (see Table 1) using 10 mol% of the cationic rhodium complex [Rh(cod)₂]BF₄ with a set of different bisphosphine-based ligands in THF/CH₂Cl₂ 4:1 at 40 °C. An array of bisphosphines, BINAP, tol-BINAP, BIPHEP, DPEphos, and Xantphos, were tested without any defined product being obtained (see Table S1 in the SI for experimental details). The formation of a new compound was only observed when we switched to the SegPhos-type family of ligands, with (*R*)-DTBM-Segphos providing the largest amounts of the new product (Table 1, entries 1–3). A careful analysis of the NMR data and MS spectra revealed that the new compound was not analogous to the fused 6,7-membered ring obtained in

Table 1. Optimization of the reaction conditions.^[a]

Entry	[Rh] complex/ Ligand	Additive	Eq. 2 a	Yield of 3 a (%)
1 ^[b,c]	[Rh(cod) ₂]BF ₄ / Segphos	–	50	10
2 ^[b,c]	[Rh(cod) ₂]BF ₄ / DM-Segphos	–	50	14
3 ^[b]	[Rh(cod) ₂]BF ₄ / (<i>R</i>)-DTBM-Segphos	–	50	57
4	[Rh(cod)₂]BF₄/ (<i>R</i>)-DTBM-Segphos	–	50	54
5	[Rh(cod) ₂]BF ₄ / (<i>R</i>)-DTBM-Segphos	–	40	41
6 ^[d]	[Rh(cod) ₂]BF ₄ / (<i>R</i>)-DTBM-Segphos	–	25	32 ^[e]
7	[Rh(cod)Cl] ₂ / (<i>R</i>)-DTBM-Segphos	AgSbF ₆	50	45 ^[e]
8	[Rh(cod)Cl] ₂ / (<i>R</i>)-DTBM-Segphos	AgPF ₆	50	39 ^[e]
9	[Rh(cod)Cl] ₂ / (<i>R</i>)-DTBM-Segphos	NaBARF	50	27 ^[e]
10	–/–	–	50	No rx.

^[a] Unless otherwise noted, reactions were carried out with 0.09 mmol of **1 a** ($[1 \mathbf{a}] = 8.5 \text{ mM}$), at room temperature in 10 mL of THF/DCM 4:1.

^[b] Reaction carried at 40 °C.

^[c] Traces of cyclotrimerization product of DMAD were detected.

^[d] $[1 \mathbf{a}] = 32 \text{ mM}$ instead of 8.5 mM.

^[e] Yields obtained by ¹H-NMR using mesitylene as the internal standard.

our previous studies with alkenes (Scheme 1d) but was rather a *cis*-3,4-arylvinylyl substituted pyrrolidine derivative. This new compound was identified as **3 a**, which is constituted by two units of **2 a** (DMAD) and one unit of the 1,5-bisallene **1 a**. Remarkably, the process seems to be completely diastereoselective and only the *cis* isomer was formed. However, although a chiral ligand was used, no enantioinduction was observed. The structure and stereochemistry of **3 a** were unambiguously confirmed by X-ray crystallographic analysis (Figure 1).

Pyrrolidine derivatives are one of the most commonly found nitrogen heterocycles in drug fragments.^[43] Moreover, the vinyl substituent in the heterocyclic compound could be further elaborated or may impart interesting physico-chemical properties. Given the great demand in both organic and medicinal

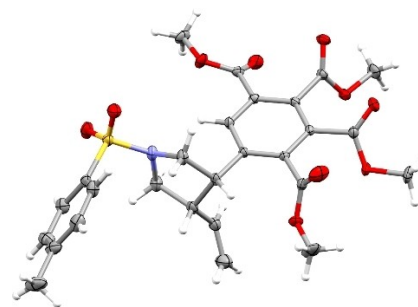


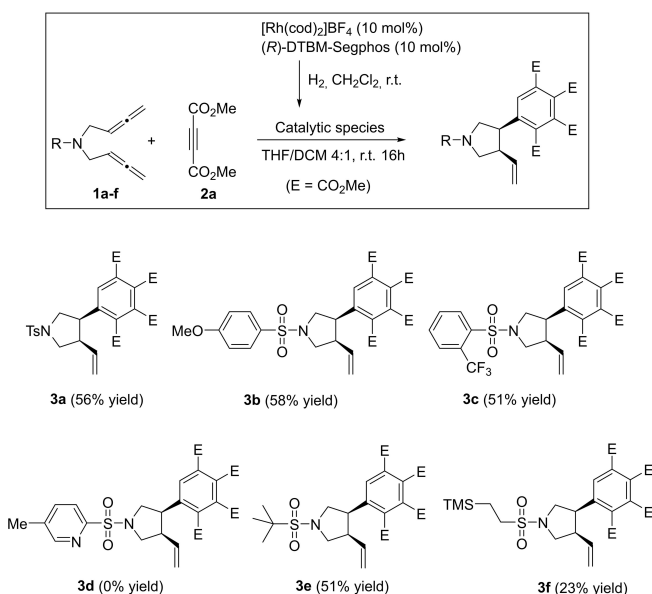
Figure 1. ORTEP representation of **3 a** at 50% of probability level CCDC 2098127.

chemistry to find new methods to construct these vinylpyrrolidine derivatives,^[43–44] and the new reactivity pattern observed we were very interested in exploring this new cyclization process in depth, so we proceeded to further optimize the reaction.

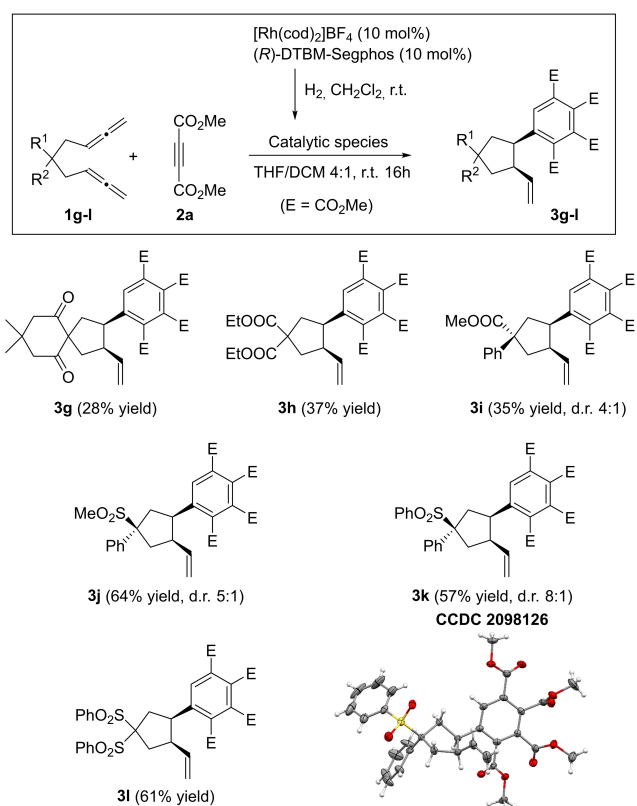
The cyclotrimerization product of DMAD was also identified with a significant 8% yield at 40 °C using (*R*)-DTBM-Segphos as a ligand (Table 1, entry 3). To our delight, performing the reaction at room temperature (Table 1, entry 4) avoided the formation of the cyclotrimerization byproduct without having a detrimental impact on the production of **3 a**.

We then carried out a solvent screening (see Table S2 in the SI) that showed that the initial mixture THF/CH₂Cl₂ 4:1 was better than CH₂Cl₂, THF, acetonitrile, toluene:CH₂Cl₂ 4:1, and dichloroethane for a process such as this. Reducing the amount of DMAD **2 a** from 50 equiv. to 40 equiv. (Table 1, entry 5) resulted in a lower yield of **3 a**. In another attempt to reduce the amount of DMAD, the reaction was set up with 25 equiv. of DMAD and an increased concentration (Table 1, entry 6) but this did not improve the outcome either. Other concentrations of bisallene **3 a** and equivalents of alkyne **2 a** were also tested but no better results were obtained (see Table S3 in SI). Larger counter ions for cationic rhodium were studied using the complex [Rh(cod)Cl]₂ together with different silver and sodium salts (Table 1, entries 7–9) but no better results were observed (see Table S4 in the SI for other catalytic systems tested). A blank experiment was also run in the absence of any catalytic system demonstrating the role of the rhodium in the cyclization process (Table 1, entry 10). Therefore, the optimal reaction conditions for further studies were defined as **1 a** ($[1 \mathbf{a}] = 8.5 \text{ mM}$), dimethyl acetylenedicarboxylate **2 a** (50 equiv.), [Rh(cod)₂]BF₄ (10 mol%), (*R*)-DTBM-SegPhos (10 mol%) in THF/CH₂Cl₂ 4:1 at room temperature for 16 hours (Table 1, entry 4). When the optimized reaction conditions were applied with 1 mmol rather than 0.09 mmol of starting material, the yield of **3 a** was found to be 41%.

Having established the most suitable reaction conditions, the scope of the new cyclization reaction was tested with a series of sulfonamide-tethered bis-allenes **1b–1f** (Scheme 2). Bisallenes with aryl sulfonamides



Scheme 2. Substrate scope of sulfonamide-tethered bisallenes **1a–1f**.



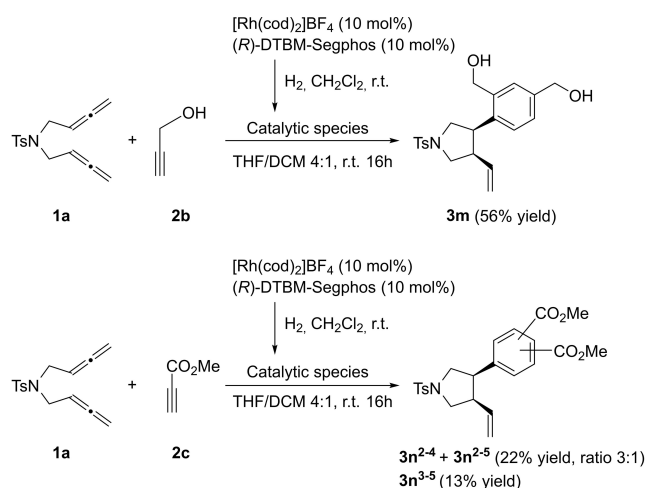
Scheme 3. Substrate scope of carbon-tethered bisallenes **1g–1l**.

with different electronically demanding substituents in *para* and *ortho* positions (**1a**, **1b**, and **1c**) successfully afforded the corresponding pyrrolidines (**3a**, **3b**, and **3c**). Bisallenes with non-aryl sulfonamide tethers such as **1e** and **1f** were also active in the process affording pyrrolidine derivatives **3e** and **3f** in moderate to good yields. The cyclization process did not proceed with the pyridine sulfonamide-tethered bisallene **1d** probably due to the presence of a potentially coordinating nitrogen atom which might poison or interfere with the rhodium catalyst.

We then tried to broaden the scope of this cyclization reaction with bisallenes tethered with disubstituted carbon atoms in order to obtain *cis*-3,4-arylvinylcyclopentane derivatives (Scheme 3). The cyclopentane skeleton is also present in a large number of biologically active molecules. Moreover, vinyl-substituted cyclopentanes are amenable to a wide range of synthetic transformations and can play a valuable role as building blocks.^[44] Using substrates with a carbonyl group in the quaternary carbon atom of the tether of the 1,5-bisallenes yielded moderate yields of the corresponding *cis*-3,4-disubstituted cyclopentanes **3g**, **3h**, and **3i**. In contrast, when the carbonyl group was substituted for an alkyl or arylsulfonyl group, better yields of derivatives **3j–3l** were obtained. Derivatives **3i**, **3j**, and **3k** were obtained as a mixture of diastereomers, the ratio of which was determined by ¹H NMR spectroscopy. The assignment of the major and minor isomer was determined by NOESY experiments. The cross peaks between the two *cis* protons of the cyclopentane with the protons of the phenyl ring of the tether allowed us to distinguish between major and minor isomers (see SI). In addition, the stereochemistry of the major isomer of **3k** was unambiguously confirmed by X-ray crystallographic analysis (Scheme 3).

To further extend the substrate scope, two mono-substituted alkynes **2b** and **2c** were tested with NTs-tethered bisallene **1a** (Scheme 4). With propargylic alcohol **2b** the reaction was completely regioselective and only the 2,4-regioisomer was obtained in a 56% yield. ¹H NMR spectroscopy confirmed the formation of a single regioisomer **3m**, which was identified by NMR experiments (see SI). In contrast, with methyl propiolate **2c** mixtures of three regioisomers (**3n²⁻⁴**, **3n²⁻⁵** and **3n³⁻⁵**) were found in a 35% overall yield.

To gain understanding of the reaction mechanism, we evaluated the process that transforms **1a** and **2a** into **3a** computationally. The Gibbs energy profiles computed at 298 K and 1 atm with the M06L–D3/ccpVTZ-PP/SMD(76% THF, 24% CH₂Cl₂)^[45]//B3LYP–D3/ccpVDZ-PP method are depicted in Figure 2 and Figure 3, the molecular structures of the TSs in Figures S4 and S5, and the whole catalytic cycle is shown in Scheme 5. To reduce the computational effort required, (R)-SegPhos was chosen as the model



Scheme 4. Scope with respect to two different alkynes **2b** and **2c**.

phosphine ligand instead of the optimal ligand (*R*)-DTBM-Segphos (see SI for a complete description of the computational methods). Among the different coordination possibilities of the 1,5-bisallene, we decided to study only those that could lead to the formation of the product obtained in the experiments.

The first part of the reaction follows the typical [2+2+2] reaction mechanism.^[46] It starts with the coordination equilibrium between DMAD (**A1**) and 1,5-bisallene (**A1'**) with the active rhodium catalyst, with the formation of **A1** being the most exergonic

process, releasing $14.6 \text{ kcal} \cdot \text{mol}^{-1}$. From **A1**, either a second DMAD unit or one of the distal double bonds of the 1,5-bisallene can coordinate to the rhodium. The incorporation of the second DMAD unit generates **A2** at a cost of $3.7 \text{ kcal} \cdot \text{mol}^{-1}$. On the other hand, two possible coordination orientations of the 1,5-bisallene lead to **A2'** and **A2''**, at costs of 4.5 and $6.4 \text{ kcal} \cdot \text{mol}^{-1}$, respectively. For the upcoming oxidative cyclometalation, both the distal and the central carbon of the allene moiety can bind to Rh. Since **A2**, **A2'**, and **A2''** are in equilibrium, the major rhodacyclo intermediate should be the one coming from the lowest energy transition state among the five possible paths in accordance with the Curtin–Hammett principle.^[47] The most favourable path is the $\text{C}_{\text{sp}2}\text{--C}_{\text{sp}3}$ bond formation from orientation **A2'**, overcoming a total Gibbs energy barrier of $11.4 \text{ kcal} \cdot \text{mol}^{-1}$ through **TS'(A2'A3)** and giving the rhodacyclopentene **A3**. This step **A1**→**A3** is exergonic by $26.8 \text{ kcal} \cdot \text{mol}^{-1}$. In this study, the oxidative coupling between the allene moiety and the alkyne is preferred over the alkyne–alkyne coupling (**TS(A2 A3)**, $\Delta G^\ddagger = 19.0 \text{ kcal} \cdot \text{mol}^{-1}$).^[35–38]

The coordination of DMAD to **A3** gives **A4**, a 16-electron square-pyramidal complex. The subsequent $\text{C}\equiv\text{C}$ insertion (Schore mechanism^[48]) is preferred to occur in the equatorial Rh–C bond (**TS'(A4 A5)**) to produce the conjugated rhodacycloheptadiene **A5**. This process has a total Gibbs energy barrier of $16.5 \text{ kcal} \cdot \text{mol}^{-1}$ and is exergonic by $15.7 \text{ kcal} \cdot \text{mol}^{-1}$. The reductive elimination of **A5** leads to **A6** through **TS(A5 A6)**, surpassing a Gibbs energy barrier of

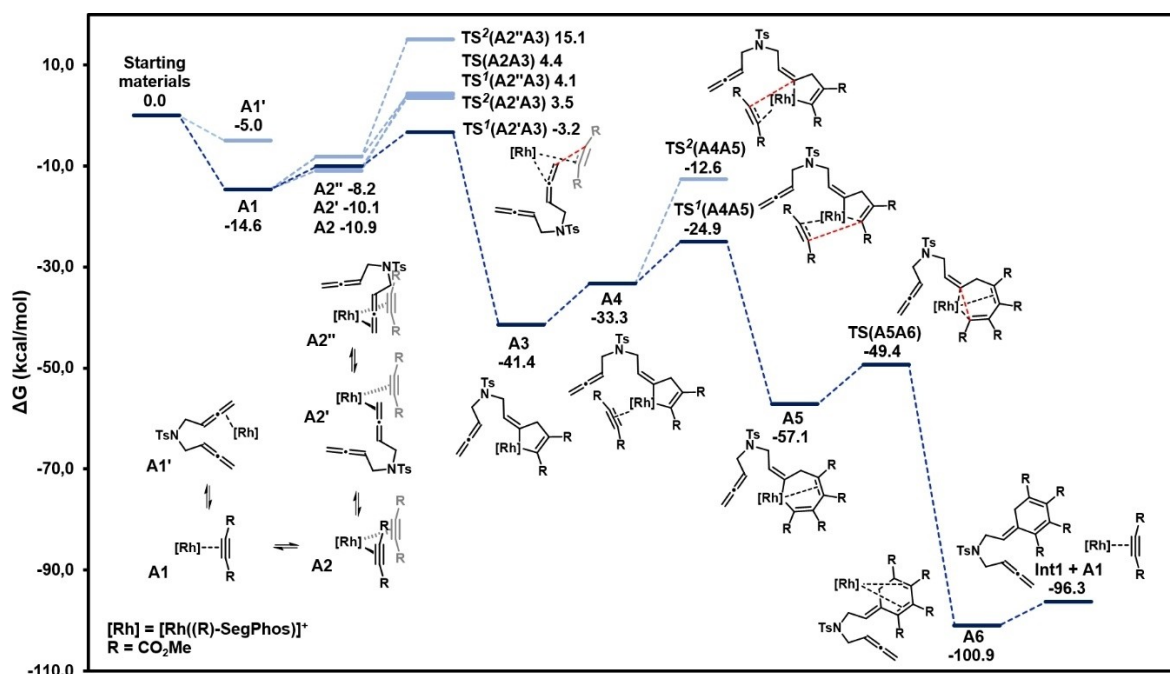


Figure 2. Gibbs energy profile (in $\text{kcal} \cdot \text{mol}^{-1}$) for the [2+2+2] cycloaddition of 1,5-bisallene **1a** and dimethyl acetylenedicarboxylate (DMAD) **2a** leading to **Int1**.

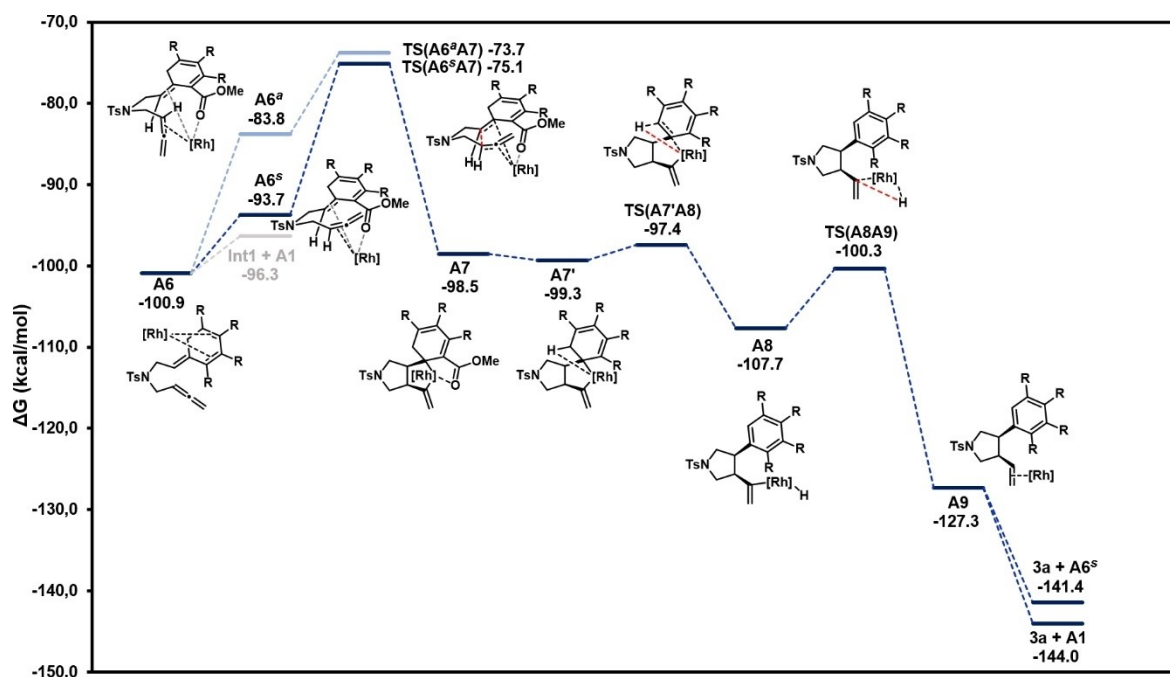
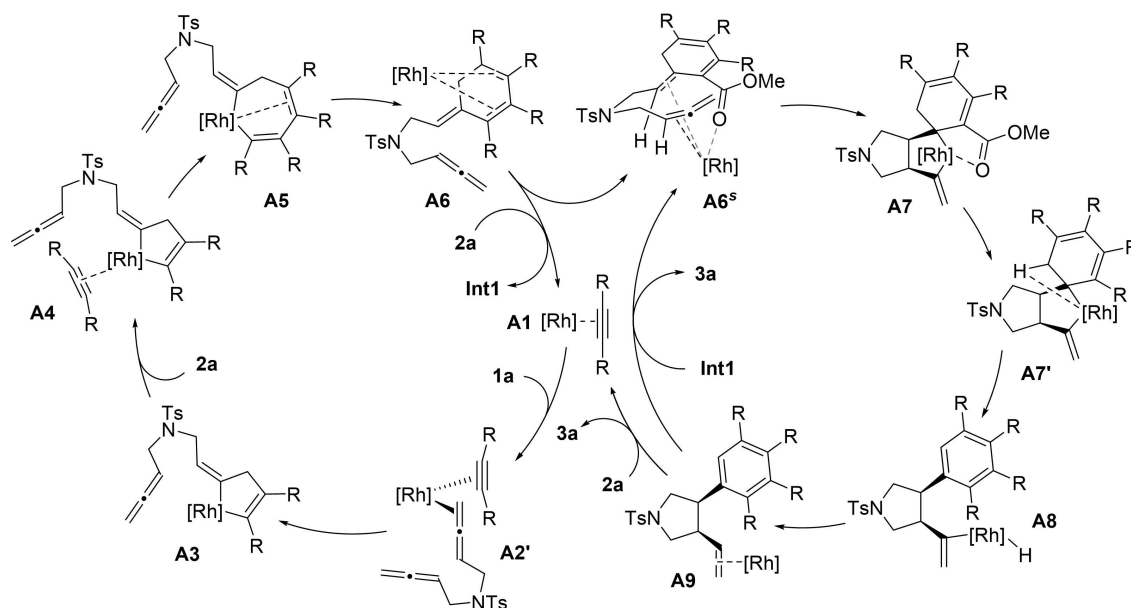


Figure 3. Gibbs energy profile (in kcal·mol⁻¹) for the cycloisomerization of **Int1** leading to **3a**.



Scheme 5. Catalytic cycle for the cascade cyclization reaction of 1,5-bisallene **1a** and dimethyl acetylenedicarboxylate (DMAD) **2a** leading to **3a**.

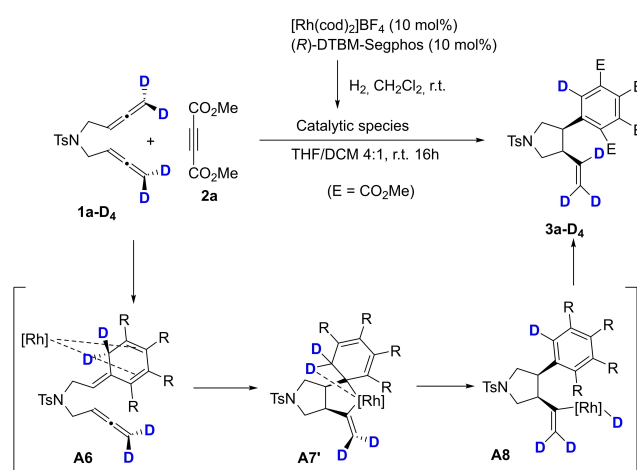
7.7 kcal·mol⁻¹ and releasing 43.8 kcal·mol⁻¹. **A6** exhibits a distorted square-planar geometry in which the two cyclic double bonds are η^2 -coordinated to the rhodium centre ($d_{\text{Rh-C}} = 2.317, 2.136, 2.216$ and 2.275 Å). Intermediate **A6** can now release the catalyst to give **Int1** at a cost of 4.6 kcal·mol⁻¹ to reinitiate the cycle on the left in Scheme 5. Alternatively, it can rearrange into **A6^s**, an 18-electron complex to start the

catalytic cycle on the right of Scheme 5. In **A6^s** one of the carboxylate oxygens occupies a coordinating position ($d_{\text{Rh-O}} = 2.219$ Å) and is η^2 -coordinated to the exocyclic double bond and to the internal double bond of the remaining allene moiety. This intermediate evolves to the *syn*-fused rhodacyclopentane **A7** by oxidative cyclometalation. The combined Gibbs energy barrier for the rearrangement and the oxidative

coupling transition state (**TS(A6^sA7)**) is 25.8 kcal·mol⁻¹ and is slightly endergonic by 2.4 kcal·mol⁻¹. The transition state leading to the *anti*-fused rhodacyclopentane has a higher energy barrier of 27.2 kcal·mol⁻¹ (**TS(A6^aA7)**). The exocyclic double bond isomerization from **A6** was also evaluated. However, the process present an energy barrier of 29.5 Kcal/mol, which is higher than the barrier from **A6** to **A7** (see Figure S6 in the SI). **A7** easily rearranges into **A7'**, creating an agostic interaction between the hydrogen of 6-membered ring and rhodium ($d_{\text{Rh-H}} = 1.74 \text{ \AA}$), and evolves to **A8** through a β -hydride elimination mechanism. This step has a low Gibbs energy barrier of 1.9 kcal·mol⁻¹ (**TSA7'A8**) and is exergonic by 8.4 kcal·mol⁻¹. Finally, **A9** is obtained after a reductive elimination (**TS(A8 A9)**, $\Delta G^\ddagger = 7.4 \text{ kcal}\cdot\text{mol}^{-1}$) releasing 19.6 kcal·mol⁻¹. Subsequent release of the Rh(I) complex leads to **3a** and completes the catalytic cycle.

In summary, the complete reaction mechanism that leads to compound **3a** (Figure 2 and Figure 3) has an overall reaction energy of $-129.4 \text{ kcal}\cdot\text{mol}^{-1}$ ($\Delta G = G_{3a} - [G_{1a} + 2 G_{2a}]$) and has an energetic span between the turnover frequency (TOF) determining intermediate (TDI, **A6**) and the TOF determining transition state (TDTS, **TS(A6^sA7)**) of 25.8 kcal·mol⁻¹.^[49-50]

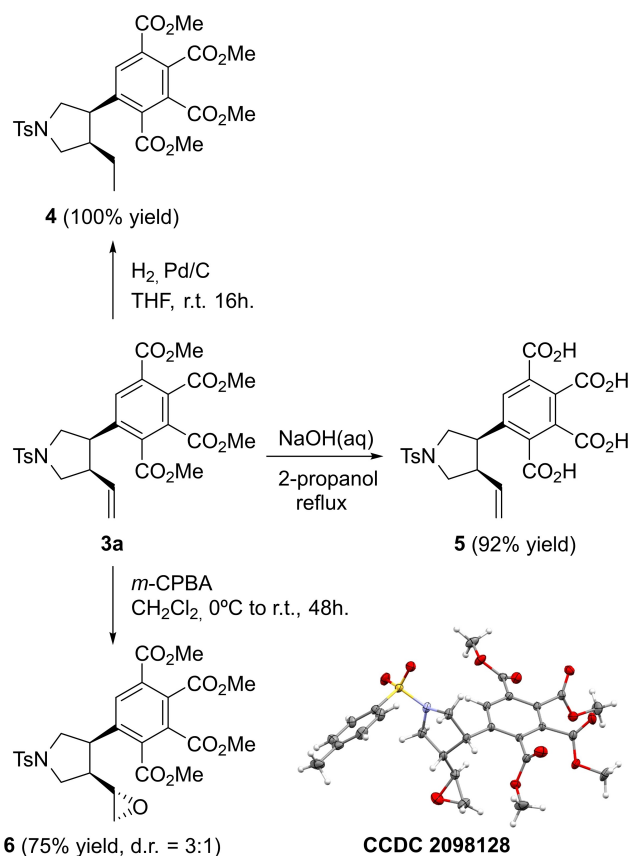
In order to obtain experimental evidence of the proposed mechanism, we performed the reaction starting with deuterated bisallene **1a-D₄** (Scheme 6). Under the optimized reaction conditions, **3a-D₄** was obtained with a 26% yield. The deuterated product was fully characterized by NMR spectrometry and MS spectroscopy (see SI). This experiment confirms the transfer of a **D** atom to the internal position of the double bond through a β -hydride elimination and subsequent reductive elimination. In Scheme 6 inter-



Scheme 6. Deuterium-labelling experiment for the cascade reaction of bisallene **1a-D₄** and **2a**.

mediates **A6**, **A7'** and **A8** are drawn to better illustrate the process.

To demonstrate potential synthetic utilities of this protocol several further transformations were evaluated for product **3a**. The vinyl double bond of pyrrolidine **3a** was both hydrogenated with bubbling H_2 at atmospheric pressure in the presence of Pd/C catalyst and epoxidated using meta-chloroperbenzoic acid. The corresponding derivatives **4** and **6** were obtained in excellent yields (Scheme 7). Epoxide **6** was obtained as a 3:1 diastereomeric mixture and the structure of the major isomer was identified by X-ray diffraction analysis. Hydrolysis of the four ester groups in the aromatic ring was carried out using an aqueous solution of sodium hydroxide in refluxing 2-propanol to afford a 92% yield of tetra acid derivative **5**. This process opens the door to the generation of dianhydride derivatives for the preparation of polyimide polymers, which are important compounds in membrane technology.^[51-52] In addition, dianhydride monomers together with the vinyl group could generate cross-linked polymers with interesting properties.



Scheme 7. Further functionalization of **3a**.

Conclusion

In summary, we have developed an efficient and a diastereoselective method for the rapid construction of *cis* 3,4-arylvinyl pyrrolidine and cyclopentane derivatives through a new cycloaddition process of 1,5-bisallenes and alkynes under rhodium catalysis. The complete mechanism of this transformation has been rationalized by DFT calculations and experimentally. The global process encompasses a Rh-catalyzed [2 + 2 + 2] cycloaddition between two units of alkyne and one unit of allene, followed by a cycloisomerization reaction involving the second allene unit in the molecule affording the disubstituted arylvinylcyclic derivative.

Experimental Section

General Procedure for the Synthesis of Derivatives 3a–3l

In a 10 mL capped vial, a mixture of [Rh(cod)₂]BF₄ (3.7 mg, 0.009 mmol) and (*R*)-DTBM-Segphos (11.3 mg, 0.01 mmol) was purged with nitrogen and dissolved in anhydrous CH₂Cl₂ (4 mL). Hydrogen gas was bubbled into the catalyst solution and the mixture was stirred for 30 minutes. The resulting mixture was concentrated to dryness under a stream of hydrogen, dissolved again in anhydrous CH₂Cl₂ (2 mL) and transferred via syringe into a solution of bisallene **1a** (25 mg, 0.09 mmol, 1 equiv.) and dimethyl acetylenedicarboxylate **2a** (0.56 mL, 4.54 mmol, 50 equiv.) in anhydrous THF (8 mL) under inert atmosphere at room temperature. The resulting mixture was stirred for 16 hours. The solvent was removed under reduced pressure and the crude reaction mixture was purified by column chromatography on silica gel using mixtures of hexane/EtOAc as the eluent (90:10 to 30:70 v/v) to afford compound **3a** (28.4 mg, 56% yield) as a colourless solid.

Compound 3a. (28.4 mg, 56% yield, colourless solid). MW (C₂₇H₂₉NO₁₀S): 559.59 g/mol; Rf: 0.23 (Hexane/EtOAc 6:4); MP (°C): 166–167; IR (ATR) ν (cm⁻¹): 2952, 1742, 1722, 1240, 1215, 1159; ¹H NMR (400 MHz, CDCl₃) δ (ppm): 2.46 (s, 3H), 2.91–2.99 (m, 1H), 3.42 (dd, ²*J* = 10.5 Hz, ³*J* = 5.3 Hz, 1H), 3.53 (dd, ²*J* = 10.5 Hz, ³*J* = 7.1 Hz, 1H), 3.61–3.67 (m, 3H), 3.81 (s, 3H), 3.84 (s, 3H), 3.92 (s, 3H), 3.93 (s, 3H), 4.84 (d, ³*J*_{trans} = 17.0 Hz, 1H), 4.90 (d, ³*J*_{cis} = 10.3 Hz, 1H), 5.19–5.30 (m, 1H), 7.36 (d, ³*J*_{ortho} = 8.2 Hz, 2H), 7.77 (d, ³*J*_{ortho} = 8.2 Hz, 2H), 7.94 (s, 1H); ¹³C NMR (101 MHz, CDCl₃) δ (ppm): 21.70, 44.04, 46.56, 51.60, 51.87, 52.96, 53.16, 53.29, 53.36, 118.65, 127.69, 130.01, 130.20, 130.22, 131.92, 133.88, 133.96, 134.17, 137.34, 138.69, 144.01, 164.87, 165.74, 167.30, 167.43; ESI-HRMS (m/z) calcd for [M + Na]⁺ = 582.1404; found 582.1404.

Compound 3b. (30.2 mg, 58% yield, colourless oil). MW (C₂₇H₂₉NO₁₁S): 575.59 g/mol; Rf: 0.19 (Hexanes/EtOAc 6:4); IR (ATR) ν (cm⁻¹): 2951, 1728, 1243, 1206, 1155; ¹H NMR (400 MHz, CDCl₃) δ (ppm): 2.92–3.02 (m, 1H), 3.40 (dd, ²*J* = 10.5 Hz, ³*J* = 5.4 Hz, 1H), 3.52 (dd, ²*J* = 10.5 Hz, ³*J* = 7.1 Hz, 1H), 3.59–3.70 (m, 3H), 3.81 (s, 3H), 3.84 (s, 3H), 3.90 (s, 3H), 3.91 (s, 3H), 3.93 (s, 3H), 4.85 (dt, ³*J*_{trans} = 17.1 Hz, ⁴*J* = ²*J* = 1.1 Hz, 1H), 4.91 (dt, ³*J*_{cis} = 10.5 Hz, ⁴*J* = ²*J* = 1.1 Hz, 1H), 5.25

(ddd, ³*J*_{trans} = 17.1 Hz, ³*J*_{cis} = 10.5 Hz, ³*J* = 8.2 Hz, 1H), 7.00–7.06 (m, 2H), 7.80–7.85 (m, 2H), 7.91 (s, 1H); ¹³C NMR (101 MHz, CDCl₃) δ (ppm): 44.04, 46.59, 51.69, 51.88, 52.99, 53.17, 53.30, 53.38, 55.78, 114.55, 118.66, 128.55, 129.80, 130.19, 130.24, 131.92, 133.93, 134.14, 137.36, 138.78, 163.33, 164.89, 165.76, 167.31, 167.45; ESI-HRMS (m/z) calcd for [M + Na]⁺ = 598.1353; found 598.1359.

Compound 3c. (28.4 mg, 51% yield, pale yellow oil). MW (C₂₇H₂₆F₃NO₁₀S): 613.56 g/mol; Rf: 0.26 (Hexanes/EtOAc 6:4); IR (ATR) ν (cm⁻¹): 2953, 1726, 1242, 1203, 1143; ¹H NMR (400 MHz, CDCl₃) δ (ppm): 3.12–3.21 (m, 1H), 3.53 (dd, ²*J* = 10.2 Hz, ³*J* = 5.2 Hz, 1H), 3.67 (dd, ²*J* = 10.2 Hz, ³*J* = 6.8 Hz, 1H), 3.71–3.79 (m, 2H), 3.79–3.89 (m, 1H), 3.86 (s, 3H), 3.86 (s, 3H), 3.92 (s, 3H), 3.92 (s, 3H), 4.91–5.02 (m, 2H), 5.38 (ddd, ³*J*_{trans} = 17.0 Hz, ³*J*_{cis} = 10.5 Hz, ³*J* = 8.2 Hz, 1H), 7.70–7.77 (m, 2H), 7.93 (m, 2H), 8.21–8.26 (m, 1H); ¹³C NMR (101 MHz, CDCl₃) δ (ppm): 44.32, 46.82, 51.19, 51.63, 53.08, 53.19, 53.27, 53.41, 118.95, 122.73 (q, ¹*J*_{C-F} = 274.0 Hz), 128.03 (q, ²*J*_{C-F} = 33.2 Hz), 128.72 (q, ³*J*_{C-F} = 6.4 Hz), 130.22, 130.27, 131.81, 131.92, 132.56 (q, ⁴*J*_{C-F} = 1.2 Hz), 133.03, 133.57, 134.31, 137.46, 138.37 (q, ³*J*_{C-F} = 1.3 Hz), 138.48, 164.84, 165.76, 167.35, 167.46; ESI-HRMS (m/z) calcd for [M + Na]⁺ = 636.1122; found 636.1128.

Compound 3e. (24.3 mg, 51% yield, colourless oil). MW (C₂₄H₃₁NO₁₀S): 525.57 g/mol; Rf: 0.28 (Hexanes/EtOAc 6:4); IR (ATR) ν (cm⁻¹): 2952, 1728, 1240, 1201, 1126; ¹H NMR (400 MHz, CDCl₃) δ (ppm): 1.46 (s, 9H), 3.12–3.22 (m, 1H), 3.48 (dd, ²*J* = 10.3 Hz, ³*J* = 6.0 Hz, 1H), 3.67–3.76 (m, 1H), 3.83 (dd, ²*J* = 10.3 Hz, ³*J* = 6.9 Hz, 1H), 3.86–3.97 (m, 2H), 3.86 (s, 3H), 3.87 (s, 3H), 3.918 (s, 3H), 3.924 (s, 3H), 4.98–5.05 (m, 2H), 5.32–5.43 (m, 1H), 8.03 (s, 1H); ¹³C NMR (101 MHz, CDCl₃) δ (ppm): 24.54, 44.78, 47.18, 53.05, 53.18, 53.21, 53.41, 53.60, 61.51, 118.81, 130.02, 130.32, 131.89, 133.72, 134.30, 137.52, 139.12, 164.82, 165.81, 167.33, 167.51; ESI-HRMS (m/z) calcd for [M + Na]⁺ = 548.1561; found 548.1563.

Compound 3f. (11.6 mg, 23% yield, colourless oil). MW (C₂₅H₃₅NO₁₀SSi): 569.70 g/mol; Rf: 0.35 (Hexanes/EtOAc 6:4); IR (ATR) ν (cm⁻¹): 2951, 1729, 1245, 1204, 1143; ¹H NMR (400 MHz, CDCl₃) δ (ppm): 0.08 (s, 9H), 1.06–1.13 (m, 2H), 2.96–3.03 (m, 2H), 3.14–3.23 (m, 1H), 3.48 (dd, ²*J* = 10.2 Hz, ³*J* = 5.3 Hz, 1H), 3.65–3.85 (m, 4H), 3.87 (s, 3H), 3.88 (s, 3H), 3.92 (s, 3H), 3.92 (s, 3H), 4.95–5.05 (m, 2H), 5.41 (ddd, ³*J*_{trans} = 16.6 Hz, ³*J*_{cis} = 10.8 Hz, ³*J* = 8.2 Hz, 1H), 8.01 (s, 1H); ¹³C NMR (101 MHz, CDCl₃) δ (ppm): -1.82, 10.29, 44.48, 46.98, 47.81, 51.45, 51.75, 53.09, 53.19, 53.31, 53.42, 118.89, 130.21, 130.35, 131.97, 133.77, 134.22, 137.43, 138.71, 164.90, 165.82, 167.38, 167.47; ESI-HRMS (m/z) calcd for [M + Na]⁺ = 592.1643; found 592.1645.

Compound 3g. (13.7 mg, 28% yield, colourless oil). MW (C₂₈H₃₂NO₁₀S): 528.55 g/mol; Rf: 0.30 (Hexanes/EtOAc 6:4); IR (ATR) ν (cm⁻¹): 2952, 1724, 1690, 1236, 1201, 1157; ¹H NMR (400 MHz, CDCl₃) δ (ppm): 0.95 (s, 3H), 1.08 (s, 3H), 2.21 (dd, ²*J* = 13.6 Hz, ³*J* = 4.2 Hz, 1H), 2.33–2.42 (m, 2H), 2.57 (dd, ²*J* = 10.1 Hz, ⁴*J* = 1.7 Hz, 1H), 2.60 (dd, ²*J* = 10.0 Hz, ⁴*J* = 1.7 Hz, 1H), 2.65–2.77 (m, 3H), 2.95–3.04 (m, 1H), 3.56 (dt, ³*J* = 11.7 Hz, ³*J* = 7.1 Hz, 1H), 3.85 (s, 3H), 3.90 (s, 3H), 3.92 (s, 3H), 3.93 (s, 3H), 4.76 (d, ³*J*_{trans} = 17.0 Hz, 1H), 4.81 (d, ³*J*_{cis} = 10.3 Hz, 1H), 5.44 (ddd, ³*J*_{trans} = 17.0 Hz, ³*J*_{cis} =

10.3 Hz, $^3J=8.8$ Hz, 1H), 7.99 (s, 1H); ^{13}C NMR (101 MHz, CDCl_3) δ (ppm): 27.70, 29.35, 30.73, 34.09, 39.78, 45.35, 47.99, 51.37, 52.40, 53.00, 53.09, 53.18, 53.29, 69.81, 117.34, 129.55, 129.59, 132.50, 133.78, 136.77, 137.80, 140.97, 165.27, 165.89, 167.75, 167.83, 207.35, 207.68; ESI-HRMS (m/z) calcd for $[\text{M}+\text{Na}]^+=551.1888$; found 551.1884.

Compound 3h. (18.4 mg, 37% yield, colourless oil). MW ($\text{C}_{27}\text{H}_{32}\text{NO}_{12}$): 548.54 g/mol; Rf: 0.37 (Hexanes/EtOAc 6:4); IR (ATR) ν (cm^{-1}): 2952, 1725, 1241, 1201, 1159; ^1H NMR (400 MHz, CDCl_3) δ (ppm): 1.23–1.31 (m, 6H), 2.32 (dd, $^2J=14.2$ Hz, $^3J=5.2$ Hz, 1H), 2.60 (d, $^3J=8.0$ Hz, 1H), 2.61 (d, $^3J=10.5$ Hz, 1H), 2.69 (dd, $^2J=14.2$ Hz, $^3J=7.5$ Hz, 1H), 2.97–3.05 (m, 1H), 3.59 (dt, $^3J=10.5$ Hz, $^3J=8.0$ Hz, 1H), 3.85 (s, 3H), 3.89 (s, 3H), 3.91 (s, 3H), 3.92 (s, 3H), 4.18–4.28 (m, 4H), 4.80–4.85 (m, 2H), 5.39 (ddd, $^3J_{\text{trans}}=17.8$ Hz, $^3J_{\text{cis}}=9.7$ Hz, $^3J=8.2$ Hz, 1H), 7.93 (s, 1H); ^{13}C NMR (101 MHz, CDCl_3) δ (ppm): 14.16, 14.18, 38.22, 38.88, 44.80, 46.70, 52.96, 53.08, 53.16, 53.29, 58.93, 61.93, 61.95, 116.93, 129.64, 129.65, 132.31, 133.73, 137.01, 137.74, 140.94, 165.23, 165.87, 167.69, 167.75, 172.03, 172.12; ESI-HRMS (m/z) calcd for $[\text{M}+\text{Na}]^+=571.1786$; found 571.1785.

Compound 3i. (17.2 mg, 35% yield, 4:1 ratio, colourless oil). MW ($\text{C}_{29}\text{H}_{30}\text{O}_{10}$): 538.5 g/mol; Rf: 0.42 (Hexanes/EtOAc 6:4); IR (ATR) ν (cm^{-1}): 2950, 1722, 1234, 1196, 1155; ^1H NMR (400 MHz, CDCl_3) δ (ppm): 2.04–2.14 (m, 1H, M), 2.27 (t, $^2J=^3J=12.0$ Hz, 1H, M), 2.48 (dd, $^2J=14.0$ Hz, $^3J=7.4$ Hz, 1H, m), 2.60–2.68 (m, 1H, m), 2.70–2.82 (m, 2H, m), 2.92–3.02 (m, 1H, m), 3.05–3.21 (m, 3H, M), 3.45 (ddd, $^3J=12.1$ Hz, $^3J=9.4$ Hz, $^3J=6.4$ Hz, 1H, m), 3.65 (s, 3H, M), 3.67 (s, 3H, m), 3.62–3.72 (m, 1H, M), 3.74 (s, 3H, m), 3.83 (s, 3H, m), 3.86 (s, 3H, M), 3.86 (s, 3H, M), 3.91 (s, 6H, M, 3H, m), 3.94 (s, 3H, m), 4.75–4.90 (m, 4H, M+m), 5.23–5.41 (m, 2H, M+m), 7.27–7.46 (m, 10H, M+m), 7.83 (s, 1H, M), 8.01 (s, 1H, m); ^{13}C NMR (101 MHz, CDCl_3) δ (ppm): 41.51, 42.13, 43.84, 45.40, 52.92, 53.09, 53.12, 53.30, 57.72, 115.95, 126.33, 126.97, 127.46, 128.70, 129.60, 132.59, 133.54, 137.79, 138.43, 142.29, 142.53, 165.24, 165.90, 167.75, 167.79, 175.65; ESI-HRMS (m/z) calcd for $[\text{M}+\text{Na}]^+=561.1731$; found 561.1732. (M=major diastereoisomer; m=minor diastereoisomer, ratio: 4:1).

Compound 3j. (32.6 mg, 64% yield, 5:1 ratio, colourless solid). MW ($\text{C}_{28}\text{H}_{30}\text{O}_{10}\text{S}$): 558.9 g/mol; Rf: 0.33 (Hexanes/EtOAc 5:5); MP ($^{\circ}\text{C}$): 77–78; IR (ATR) ν (cm^{-1}): 2951, 1724, 1241, 1201, 1131; ^1H NMR (400 MHz, CDCl_3) δ (ppm): 2.52 (s, 3H, m), 2.53 (s, 3H, M), 2.54–2.82 (m, 2H, m), 2.79–2.91 (m, 3H, M), 2.91–3.01 (m, 1H, M), 3.06 (t, $^2J=^3J=12.4$ Hz, 1H, M), 3.13–3.27 (m, 2H, m), 3.38–3.51 (m, 2H, M+m), 3.69 (s, 3H, M), 3.78 (s, 3H, m), 3.83 (s, 3H, M), 3.86 (s, 3H, m), 3.90 (s, 3H, m), 3.92 (s, 6H, M+m), 3.96 (s, 3H, M), 4.10–4.20 (m, 1H, m), 4.76–4.95 (m, 4H, M+m), 5.27 (ddd, $^3J_{\text{trans}}=17.0$ Hz, $^3J_{\text{cis}}=10.4$ Hz, $^3J=8.1$ Hz, 1H, m), 5.45 (ddd, $^3J_{\text{trans}}=17.2$ Hz, $^3J_{\text{cis}}=10.2$ Hz, $^3J=8.1$ Hz, 1H, M), 7.38–7.54 (m, 6H, M+m), 7.56–7.63 (m, 2H, m), 7.64–7.76 (m, 2H, M, 1H, m), 8.08 (s, 1H, M); ^{13}C NMR (101 MHz, CDCl_3) δ (ppm): 36.91, 37.65, 37.78, 43.05, 44.69, 52.79, 53.14, 53.28, 53.31, 73.79, 117.00, 128.40, 129.29, 129.39, 129.52, 129.95, 132.65, 134.10, 134.87, 137.11, 137.69, 140.70, 165.05, 165.70, 167.61, 167.70; ESI-HRMS (m/z) calcd for $[\text{M}+\text{Na}]^+=581.1452$; found

581.1443. (M=major diastereoisomer; m=minor diastereoisomer, ratio: 5:1)

Compound 3k. (31.4 mg, 57% yield, 8:1 ratio, colourless solid). MW ($\text{C}_{33}\text{H}_{32}\text{O}_{10}\text{S}$): 620.7 g/mol; Rf: 0.28 (Hexanes/EtOAc 6:4); MP ($^{\circ}\text{C}$): 194–195; IR (ATR) ν (cm^{-1}): 2953, 1728, 1246, 1200, 1140; ^1H NMR (400 MHz, CDCl_3) δ (ppm): 2.49 (dd, $^2J=14.6$ Hz, $^3J=6.1$ Hz, 1H, m), 2.64 (dd, $^2J=14.6$ Hz, $^3J=10.1$ Hz, 1H, m), 2.71–2.95 (m, 4H, M), 3.12 (t, $^2J=^3J=12.4$ Hz, 1H, M), 3.19–3.30 (m, 2H, m), 3.30–3.40 (m, 1H, M), 3.45–3.53 (m, 1H, m), 3.63 (s, 3H, M), 3.74 (s, 3H, m), 3.81 (s, 3H, M), 3.87 (s, 3H, m), 3.88 (s, 3H, m), 3.90 (s, 3H, m), 3.92 (s, 3H, M), 3.99 (s, 3H, M), 4.26–4.34 (m, 1H, m), 4.76–4.95 (m, 4H, M+m), 5.27 (ddd, $^3J_{\text{trans}}=16.5$ Hz, $^3J_{\text{cis}}=11.0$ Hz, $^3J=8.3$ Hz, 1H, m), 5.45 (ddd, $^3J_{\text{trans}}=17.3$ Hz, $^3J_{\text{cis}}=10.2$ Hz, $^3J=7.4$ Hz, 1H, M), 7.13–7.17 (m, 2H, m), 7.21–7.36 (m, 9H, M, 7H, m), 7.48–7.55 (m, 2H, M+m), 7.66 (s, 1H, m), 8.12 (s, 1H, M); ^{13}C NMR (101 MHz, CDCl_3) δ (ppm): 38.00, 38.28, 42.80, 44.45, 52.71, 53.13, 53.28, 53.30, 75.09, 116.80, 128.50, 128.50, 128.71, 128.97, 129.38, 129.68, 129.93, 132.86, 133.69, 134.01, 134.08, 136.27, 137.40, 137.75, 140.95, 165.11, 165.67, 167.58, 167.71; ESI-HRMS (m/z) calcd for $[\text{M}+\text{Na}]^+=643.1608$; found 643.1603. (M=major diastereoisomer; m=minor diastereoisomer, ratio: 8:1).

Compound 3l. (30.9 mg, 61% yield, colourless solid). MW ($\text{C}_{33}\text{H}_{32}\text{O}_{12}\text{S}_2$): 684.7 g/mol; Rf: 0.35 (Hexanes/EtOAc 6:4); MP ($^{\circ}\text{C}$): 74–75; IR (ATR) ν (cm^{-1}): 2951, 1726, 1240, 1202, 1140; ^1H NMR (400 MHz, CDCl_3) δ (ppm): 2.61 (dd, $^2J=14.9$ Hz, $^3J=6.8$ Hz, 1H), 2.69 (dd, $^2J=15.9$ Hz, $^3J=4.9$ Hz, 1H), 2.93 (dd, $^2J=15.9$ Hz, $^3J=7.9$ Hz, 1H), 3.19 (dd, $^2J=14.9$ Hz, $^3J=12.0$ Hz, 1H), 3.25–3.35 (m, 1H), 3.87 (s, 3H), 3.93 (s, 6H), 3.96 (s, 3H), 4.08 (ddd, $^3J=12.0$ Hz, $^3J=8.0$ Hz, $^3J=6.8$ Hz, 1H), 4.79–4.88 (m, 2H), 5.61 (dt, $^3J_{\text{trans}}=16.9$ Hz, $^3J_{\text{cis}}=^3J=9.8$ Hz, 1H), 7.58–7.66 (m, 4H), 7.70–7.77 (m, 2H), 7.97 (s, 1H), 8.02–8.13 (m, 4H); ^{13}C NMR (101 MHz, CDCl_3) δ (ppm): 36.57, 36.62, 44.68, 47.46, 53.15, 53.23, 53.26, 53.39, 93.35, 118.08, 128.96, 129.09, 129.34, 129.72, 131.37, 131.46, 132.44, 134.37, 134.91, 135.02, 135.46, 136.38, 136.86, 138.40, 139.49, 164.97, 165.57, 167.66, 167.74; ESI-HRMS (m/z) calcd for $[\text{M}+\text{Na}]^+=707.1227$; found 707.1220.

General Procedure for the Synthesis of Derivatives 3m–3n

In a 10 mL capped vial, a mixture of $[\text{Rh}(\text{cod})_2]\text{BF}_4$ (3.7 mg, 0.009 mmol) and (*R*)-DTBM-Segphos (11.3 mg, 0.01 mmol) was purged with nitrogen and dissolved in anhydrous CH_2Cl_2 (4 mL). Hydrogen gas was bubbled into the catalyst solution and the mixture was stirred for 30 minutes. The resulting mixture was concentrated to dryness under a stream of hydrogen, dissolved again in anhydrous CH_2Cl_2 (2 mL) and transferred via syringe into a solution of bisallene **1a** (25 mg, 0.09 mmol, 1 equiv.) and the corresponding alkyne (50 equiv.) in anhydrous THF (8 mL) under inert atmosphere at room temperature. The resulting mixture was stirred for 16 hours. The solvent was removed under reduced pressure and the crude reaction mixture was purified by column chromatography on silica gel using mixtures of hexanes/EtOAc as the eluent (95:5 to 30:70 v/v) to afford the desired compound **3**.

Compound 3m. (19.6 mg, 56% yield, colourless solid). MW ($C_{21}H_{25}NO_4S$): 387.5 g/mol; Rf: 0.53 (EtOAc); IR (ATR) ν (cm^{-1}): 3344 (br band), 2874, 1330, 1155; 1H NMR (400 MHz, $CDCl_3$) δ (ppm): 2.48 (s, 3H), 2.88–3.00 (m, 1H), 3.27 (dd, $^2J=10.0$ Hz, $^3J=8.2$ Hz, 1H), 3.54 (dd, $^2J=10.0$ Hz, $^3J=8.2$ Hz, 1H), 3.57–3.68 (m, 2H), 3.74–3.83 (m, 1H), 4.48–4.72 (m, 4H), 4.84 (d, $^3J_{cis}=10.0$ Hz, 1H), 4.91 (d, $^3J_{trans}=17.0$ Hz, 1H), 4.98–5.09 (m, 1H), 7.02 (d, $^3J_{ortho}=8.0$ Hz, 1H), 7.14 (d, $^3J_{ortho}=8.0$ Hz, 1H), 7.31 (s, 1H), 7.38 (d, $^3J_{ortho}=8.2$ Hz, 2H), 7.78 (d, $^3J_{ortho}=8.2$ Hz, 2H); ^{13}C NMR (101 MHz, $CDCl_3$) δ (ppm): 21.73, 42.33, 47.09, 51.59, 53.29, 63.56, 64.89, 117.95, 126.99, 127.45, 127.54, 127.67, 129.98, 134.06, 135.21, 136.98, 138.98, 139.78, 143.84; ESI-HRMS (m/z) calcd for $[M+Na]^+$ = 410.1397; found 410.1399.

Compound 3n. ($3n^{2+}+3n^{2-5}$, 8.7 mg, 22% yield, yellow oil; $3n^{3-5}$, 5.3 mg, 13% yield, yellow oil). MW ($C_{23}H_{25}NO_6S$): 443.5 g/mol; Rf: 0.63 (Hexane/EtOAc 6:4); IR (ATR) ν (cm^{-1}) ($3n^{2+}+3n^{2-5}$): 950, 1719, 1239, 1157; Although the 1H and ^{13}C -NMR spectra are recorded for the inseparable mixture of $3n^{2+}+3n^{2-5}$, the two spectra are described separately for clarity: 1H NMR (400 MHz, $CDCl_3$) δ (ppm) $3n^{2+}$: 2.48 (s, 3H), 3.00–3.10 (m, 1H), 3.30 (dd, $^2J=10.4$ Hz, $^3J=7.2$ Hz, 1H), 3.54 (dd, $^2J=10.4$ Hz, $^3J=7.4$ Hz, 1H), 3.60 (dd, $^2J=10.2$ Hz, $^3J=7.1$ Hz, 1H), 3.68 (dd, $^2J=10.2$ Hz, $^3J=5.1$ Hz, 1H), 3.85 (s, 3H), 3.93 (s, 3H), 4.56 (dt, $^3J=7.1$ Hz, $^3J=5.1$ Hz, 1H), 4.73–4.84 (m, 2H), 5.09 (ddd, $^3J_{trans}=17.9$ Hz, $^3J_{cis}=9.9$ Hz, $^3J=8.2$ Hz, 1H), 7.27 (d, $^3J_{ortho}=8.3$ Hz, 1H), 7.38 (d, $^3J_{ortho}=8.3$ Hz, 2H), 7.79 (d, $^3J_{ortho}=8.3$ Hz, 2H), 8.01 (dd, $^3J_{ortho}=8.3$ Hz, $^4J_{meta}=1.9$ Hz, 1H), 8.47 (d, $^4J_{meta}=1.9$ Hz, 1H); 1H NMR (400 MHz, $CDCl_3$) δ (ppm) $3n^{2-5}$: 2.46 (s, 3H), 3.00–3.11 (m, 1H), 3.37 (dd, $^2J=10.4$ Hz, $^3J=5.4$ Hz, 1H), 3.50–3.74 (m, 3H), 3.85 (s, 3H), 3.95 (s, 3H), 4.36 (q, $^3J=7.2$ Hz, 1H), 4.73–4.83 (m, 2H), 5.13–5.24 (m, 1H), 7.34–7.39 (m, 2H), 7.79 (d, $^3J_{ortho}=8.3$ Hz, 2H), 7.85 (d, $^3J_{ortho}=8.5$ Hz, 1H), 7.89–7.96 (m, 2H); 1H NMR (400 MHz, $CDCl_3$) δ (ppm) $3n^{3-5}$: 2.46 (s, 3H), 2.96–3.08 (m, 1H), 3.41 (dd, $^2J=10.2$ Hz, $^3J=5.1$ Hz, 1H), 3.49 (q, $^3J=7.1$ Hz, 1H), 3.61 (m, 2H), 3.77 (dd, $^2J=9.9$ Hz, $^3J=7.1$ Hz, 1H), 3.94 (s, 6H), 4.86 (d, $^3J_{trans}=16.9$ Hz, 1H), 4.88 (d, $^3J_{cis}=10.0$ Hz, 1H), 5.15 (ddd, $^3J_{trans}=16.9$ Hz, $^3J_{cis}=10.0$ Hz, $^3J=8.3$ Hz, 1H), 7.37 (d, $^3J_{ortho}=8.2$ Hz, 2H), 7.80 (d, $^3J_{ortho}=8.2$ Hz, 2H), 7.94 (d, $^4J_{meta}=1.6$ Hz, 2H), 8.53 (t, $^4J_{meta}=1.6$ Hz, 1H); ^{13}C NMR (101 MHz, $CDCl_3$) δ (ppm) $3n^{2+}$: 21.72, 43.11, 46.64, 51.44, 52.44, 52.50, 117.71, 127.70, 128.29, 128.83, 130.01, 130.85, 131.80, 132.79, 133.95, 134.58, 143.90, 145.38, 166.11, 167.39; ^{13}C NMR (101 MHz, $CDCl_3$) δ (ppm) $3n^{2-5}$: 21.72, 43.46, 46.41, 51.53, 51.95, 52.55, 52.69, 117.66, 127.73, 127.93, 129.02, 129.96, 130.63, 133.02, 134.24, 134.86, 139.73, 143.78, 166.22, 167.65; ^{13}C NMR (101 MHz, $CDCl_3$) δ (ppm) $3n^{3-5}$: 21.73, 46.89, 47.39, 51.15, 51.98, 52.61, 118.35, 127.69, 129.48, 130.02, 130.91, 133.53, 134.34, 136.68, 138.66, 139.35, 166.21; ESI-HRMS (m/z) ($3n^{2+}+3n^{2-5}$): calcd for $[M+Na]^+$ = 466.1295; found 466.1289.

Synthesis of Derivative 4

In a 10 mL capped vial, a mixture of **3a** (8.0 mg, 0.014 mmol) and Pd/C (10% wt, 2.0 mg, 0.002 mmol) was dissolved in THF (2 mL). Hydrogen gas was bubbled into the mixture for 20 minutes and THF was constantly added to avoid dryness. After stirring for 16 hours under hydrogen atmosphere, the

mixture was filtered through celite to remove the Pd/C. Concentration of the resulting solution under reduced pressure afforded compound **4** (8 mg, quant. yield) as a colourless solid.

Compound 4. (8.0 mg, 100% yield, colourless solid). MW ($C_{27}H_{31}NO_{10}S$): 561.60 g/mol; Rf: 0.26 (Hexane/EtOAc 6:4); MP ($^{\circ}C$): 166–167; IR (ATR) ν (cm^{-1}): 2953, 1739, 1724, 1241, 1216, 1159; 1H NMR (400 MHz, $CDCl_3$) δ (ppm): 0.66–0.78 (m, 4H), 0.93–1.12 (m, 1H), 2.12–2.24 (m, 1H), 2.46 (s, 3H), 3.24 (dd, $^2J=10.4$ Hz, $^3J=6.5$ Hz, 1H), 3.49–3.60 (m, 4H), 3.84 (s, 3H), 3.85 (s, 3H), 3.92 (s, 3H), 3.93 (s, 3H), 7.35 (d, $^3J_{ortho}=8.2$ Hz, 2H), 7.77 (d, $^3J_{ortho}=8.2$ Hz, 2H), 7.97 (s, 1H); ^{13}C NMR (101 MHz, $CDCl_3$) δ (ppm): 12.59, 21.73, 21.94, 43.57, 44.53, 51.81, 52.46, 53.13, 53.19, 53.33, 53.41, 127.73, 129.96, 130.00, 130.42, 131.91, 133.94, 134.16, 137.49, 139.81, 143.94, 164.91, 165.72, 167.47, 167.50; ESI-HRMS (m/z) calcd for $[M+Na]^+$ = 584.1561; found 584.1557.

Synthesis of Tetraacid Derivative 5

A suspension of **3a** (30 mg, 0.054 mmol) in 2-propanol (30 mL) was added to a solution of sodium hydroxide (36 mg, 0.9 mmol) in H_2O (15 mL) at room temperature. The mixture was heated to reflux and stirred for 48 hours. The solution was allowed to cool down to room temperature and the 2-propanol was evaporated under reduced pressure. HCl 1 M was then added and the aqueous mixture was washed with CH_2Cl_2 (15 mL) and extracted with diethyl ether (3×15 mL). The combined ether fractions were dried over anhydrous Na_2SO_4 , filtered and concentrated under reduced pressure to afford **5** (24.8 mg, 92% yield) as a colourless oil.

Compound 5. (24.8 mg, 92% yield, colourless oil). MW ($C_{23}H_{21}NO_{10}S$): 503.48 g/mol; IR (ATR) ν (cm^{-1}): 3468, 3063, 2918, 2628, 1706; 1H NMR (400 MHz, THF- d_8) δ (ppm): 2.42 (s, 3H), 3.03–3.11 (m, 1H), 3.36 (dd, $^2J=10.4$ Hz, $^3J=4.7$ Hz, 1H), 3.52 (dd, $^2J=10.4$ Hz, $^3J=7.0$ Hz, 1H), 3.55–3.62 (m, 1H), 3.66 (dd, $^2J=9.9$ Hz, $^3J=7.3$ Hz, 1H), 3.75 (q, $^3J=7.3$ Hz, 1H), 4.75–4.87 (m, 2H), 5.35 (ddd, $^3J_{trans}=17.1$ Hz, $^3J_{cis}=10.5$ Hz, $^3J=8.0$ Hz, 1H), 7.38 (d, $^3J_{ortho}=8.1$ Hz, 2H), 7.76 (s, 1H), 7.77 (d, $^3J_{ortho}=8.1$ Hz, 2H); ^{13}C NMR (101 MHz, THF- d_8) δ (ppm): 21.26, 44.88, 47.03, 51.84, 52.54, 117.50, 128.31, 130.25, 131.03, 131.31, 132.31, 135.11, 135.59, 135.69, 137.56, 138.34, 144.00, 166.54, 167.51, 168.03, 168.71; ESI-HRMS (m/z) calcd for $[M+Na]^+$ = 526.0778; found 526.0787.

Synthesis of Epoxide 6

In a 10 mL capped vial, **3a** (20.0 mg, 0.036 mmol) was dissolved in CH_2Cl_2 (5 mL) and 3-chloroperbenzoic acid (10 mg, 77% purity, 0.045 mmol) was added in portions at $0^{\circ}C$. The solution was allowed to warm to room temperature and was stirred for 48 hours. The solvent was removed under reduced pressure and the crude reaction mixture was purified by column chromatography on silica gel using hexanes/EtOAc mixtures as eluent (90:10 to 30:70 v/v) to obtain an inseparable diastereoisomeric mixture 3:1 of **6** (15.7 mg, 75% yield) as a colourless solid.

Compound 6. (15.7 mg, 75% yield, 3:1 ratio, colourless solid). MW ($C_{27}H_{29}NO_{11}S$): 575.58 g/mol; Rf: 0.28 (Hexanes/EtOAc 5:5); MP ($^{\circ}C$): 156–157; IR (ATR) ν (cm^{-1}): 2953, 1743, 1725,

1238, 1216, 1160; ^1H NMR (400 MHz, CDCl_3) δ (ppm): 2.16–2.27 (m, 2H, M), 2.32–2.36 (m, 1H, m), 2.36 (m, 1H, m), 2.41 (t, $^2J=^3J=4.3$ Hz, 1H, M), 2.46 (s, 3H, M), 2.44–2.51 (m, 1H, M, 5H, m), 3.28–3.33 (m, 2H, m), 3.47 (d, $^3J=6.2$ Hz, 2H, M), 3.54–3.80 (m, 6H, M+m), 3.84 (s, 6H, M+m), 3.85 (s, 3H, m), 3.86 (s, 3H, M), 3.92 (s, 3H, m), 3.92 (s, 3H, M), 3.94 (s, 6H, M+m), 7.37 (d, $^3J_{\text{ortho}}=8.0$ Hz, 4H, M+m), 7.74–7.81 (m, 4H, M+m), 8.11 (s, 1H, M), 8.13 (s, 1H, m); ^{13}C NMR (101 MHz, CDCl_3) δ (ppm) (major diastereoisomer): 21.74, 42.66, 45.20, 46.46, 49.82, 50.82, 52.20, 53.23, 53.26, 53.41, 53.47, 127.87, 130.05, 130.18, 130.64, 131.69, 133.42, 134.62, 137.51, 138.37, 144.18, 164.72, 165.50, 167.30, 167.31; ESI-HRMS (m/z) calcd for $[\text{M}+\text{Na}]^+$ = 598.1354; found 598.1357. (M = major diastereoisomer; m = minor diastereoisomer, ratio 3:1).

CCDC-2098126, CCDC-2098127 and CCDC-2098128 contain the supplementary crystallographic data for this paper. These data can be obtained free of charge from The Cambridge Crystallographic Data Centre via www.ccdc.cam.ac.uk/data_request/cif.

Acknowledgements

We are grateful for the financial support by the Spanish Ministry of Economy and Competitiveness (MINECO) (Project CTQ2017-85341-P), the UdG for a predoctoral grant to J. V. and the Generalitat de Catalunya (Project 2017-SGR-39).


References

- [1] H. F. Schuster, G. M. Coppola, Eds. *Alleney in Organic Synthesis*, Vol. 1, Wiley-Interscience, New York, 1984.
- [2] N. Krause, A. S. K. Hashmi, Eds. *Modern Allene Chemistry*, Vol. 1, Wiley-VCH, Weinheim, 2004.
- [3] F. López, J. L. Mascareñas, *Chem. Eur. J.* **2011**, *17*, 418–428.
- [4] T. Lechel, F. Pfrengle, H.-U. Reissig, R. Zimmer, *ChemCatChem* **2013**, *5*, 2100–2130.
- [5] S. Kitagaki, F. Inagaki, C. Mukai, *Chem. Soc. Rev.* **2014**, *43*, 2956–2978.
- [6] F. López, J. L. Mascareñas, *Chem. Soc. Rev.* **2014**, *43*, 2904–2915.
- [7] J. Ye, S. Ma, *Acc. Chem. Res.* **2014**, *47*, 989–1000.
- [8] A. Lledó, A. Pla-Quintana, A. Roglans, *Chem. Soc. Rev.* **2016**, *45*, 2010–2023.
- [9] R. Santhoshkumar, C.-H. Chen, *Asian J. Org. Chem.* **2018**, *7*, 1151–1163.
- [10] X.-L. Han, P.-P. Lin, Q. Li, *Chin. Chem. Lett.* **2019**, *30*, 1495–1502.
- [11] R. Bliet, M. Taillefer, F. Monnier, *Chem. Rev.* **2020**, *120*, 13545–13598.
- [12] G. Chen, X. Jiang, C. Fu, S. Ma, *Chem. Lett.* **2010**, *39*, 78–81.
- [13] B. Alcaide, P. Almendros, C. Aragoncillo, *Chem. Soc. Rev.* **2014**, *43*, 3106–3135.
- [14] H. Hopf, G. Markopoulos, *Beilstein J. Org. Chem.* **2012**, *8*, 1936–1998.
- [15] X. Jiang, X. Cheng, S. Ma, *Angew. Chem. Int. Ed.* **2006**, *45*, 8009–8013; *Angew. Chem.* **2006**, *118*, 8177–8181.
- [16] T. Kawamura, F. Inagaki, S. Narita, Y. Takahashi, S. Hirata, S. Kitagaki, C. Mukai, *Chem. Eur. J.* **2010**, *16*, 5173–5183.
- [17] S. Arai, Y. Kawata, Y. Amako, A. Nishida, *Tetrahedron Lett.* **2019**, *60*, 151168–151171.
- [18] S. M. Kim, J. H. Park, Y. K. Kang, Y. K. Chung, *Angew. Chem. Int. Ed.* **2009**, *48*, 4532–4535; *Angew. Chem.* **2009**, *121*, 4602–4605.
- [19] P. Lu, S. Ma, *Org. Lett.* **2007**, *9*, 2095–2097.
- [20] J. H. Park, E. Kim, H.-M. Kim, S. Y. Choi, Y. K. Chung, *Chem. Commun.* **2008**, 2388–2390. ■■Dear Author, if the journal has volumes, please add the journal number■■■
- [21] F. Inagaki, S. Narita, T. Hasegawa, S. Kitagaki, C. Mukai, *Angew. Chem. Int. Ed.* **2009**, *48*, 2007–2011; *Angew. Chem.* **2009**, *121*, 2041–2045.
- [22] S. Ma, P. Lu, L. Lu, H. Hou, J. Wei, Q. He, Z. Gu, X. Jiang, X. Jin, *Angew. Chem. Int. Ed.* **2005**, *44*, 5275–5278; *Angew. Chem.* **2005**, *117*, 5409–5412.
- [23] S. Ma, L. Lu, *Chem. Asian J.* **2007**, *2*, 199–204.
- [24] P. Lu, S. Ma, *Org. Lett.* **2007**, *9*, 5319–5321.
- [25] S.-K. Kang, T.-G. Baik, A. N. Kulak, Y.-H. Ha, Y. Lim, J. Park, *J. Am. Chem. Soc.* **2000**, *122*, 11529–11530.
- [26] Y.-T. Hong, S.-K. Yoon, S.-K. Kang, C.-M. Yu, *Eur. J. Org. Chem.* **2004**, 4628–4635. ■■Dear Author, if the journal has volumes, please add the journal number■■■
- [27] W. Shu, G. Jia, S. Ma, *Angew. Chem. Int. Ed.* **2009**, *48*, 2788–2791; *Angew. Chem.* **2009**, *121*, 2826–2829.
- [28] X. Lian, S. Ma, *Chem. Eur. J.* **2010**, *16*, 7960–7964.
- [29] Y. N. Lim, H.-T. Kim, H.-S. Yoon, H.-Y. Jang, *Bull. Korean Chem. Soc.* **2011**, *32*, 3117–3119.
- [30] Y. Amako, H. Hori, S. Arai, A. Nishida, *J. Org. Chem.* **2013**, *78*, 10763–10775.
- [31] C. Zhu, B. Yang, Y. Qiu, J.-E. Bäckvall, *Angew. Chem. Int. Ed.* **2016**, *55*, 14405–14408; *Angew. Chem.* **2016**, *128*, 14617–14620.
- [32] C. Zhu, B. Yang, B. K. Mai, S. Palazzotto, Y. Qiu, A. Gudmundsson, A. Rieke, F. Himo, J.-E. Bäckvall, *J. Am. Chem. Soc.* **2018**, *140*, 14324–1433.
- [33] M. T. Quirós, C. Hurtado-Rodrigo, M. P. Muñoz, *Org. Biomol. Chem.* **2017**, *15*, 6731–673.
- [34] J. Cheng, X. Jiang, S. Ma, *Org. Lett.* **2011**, *13*, 5200–5203.
- [35] A. Artigas, J. Vila, A. Lledó, M. Solà, A. Pla-Quintana, A. Roglans, *Org. Lett.* **2019**, *21*, 6608–6613.
- [36] A. Artigas, C. Castanyer, N. Roig, A. Lledó, M. Solà, A. Pla-Quintana, A. Roglans, *Adv. Synth. Catal.* **2021**, *363*, 3835–3844.
- [37] E. Haraburda, Ò. Torres, T. Parella, M. Solà, A. Pla-Quintana, *Chem. Eur. J.* **2014**, *20*, 5034–5045.
- [38] D. Cassú, T. Parella, M. Solà, A. Pla-Quintana, A. Roglans, *Chem. Eur. J.* **2017**, *23*, 14889–14899.
- [39] Z.-X. Yu, P. H.-Y. Cheong, P. Liu, C. Y. Legault, P. A. Wender, K. N. Houk, *J. Am. Chem. Soc.* **2008**, *130*, 2378–2379.

- [40] E. Haraburda, M. Fernández, A. Gifreu, J. Garcia, T. Parella, A. Pla-Quintana, A. Roglans, *Adv. Synth. Catal.* **2017**, *359*, 506–512.
- [41] E. Haraburda, A. Lledó, A. Roglans, A. Pla-Quintana, *Org. Lett.* **2015**, *17*, 2882–2885.
- [42] A. Pla-Quintana, A. Roglans, *Asian J. Org. Chem.* **2018**, *7*, 1706–1718.
- [43] E. Vitaku, D. T. Smith, J. T. Njardarson, *J. Med. Chem.* **2014**, *57*, 10257–10274.
- [44] J. Rodriguez, D. Bonne, Eds. *Stereoselective Multiple Bond-Forming Transformations in Organic Synthesis*. John Wiley & Sons, Inc. **2015**.
- [45] (76% THF, 24% CH₂Cl₂) is equivalent to a 4:1 v/v ratio of THF/CH₂Cl₂.
- [46] A. Roglans, A. Pla-Quintana, M. Solà, *Chem. Rev.* **2021**, *121*, 1894–1979.
- [47] J. I. Seeman, *Chem. Rev.* **1983**, *83*, 83–134.
- [48] N. E. Schore, *Chem. Rev.* **1988**, *88*, 1081–1119.
- [49] S. Kozuch, S. Shaik, *J. Phys. Chem. A* **2008**, *112*, 6032–6041.
- [50] S. Kozuch, S. Shaik, *Acc. Chem. Res.* **2011**, *44*, 101–110.
- [51] R. Sulub-Sulub, I. Loria-Bastarrachea, J. L. Santiago-Garcia, M. Aguilar-Vega, *RSC Adv.* **2018**, *8*, 31881–31888.
- [52] M. A. Abdulhamid, X. Ma, B. S. Ghanem, I. Pinnau, *ACS Appl. Polym. Mater.* **2019**, *1*, 63–69.
-

A Rh(I)-Catalyzed Cascade Cyclization of 1,5-Bisallenes and Alkynes for the Formation of *cis*-3,4-Arylvinylyl Pyrrolidines and Cyclopentanes

Adv. Synth. Catal. **2021**, *363*, 1–13

 J. Vila, R. Vinardell, M. Solà, A. Pla-Quintana*, A. Roglans*

